Journal of Catalysis **182,** 270–273 (1999)
Article ID jcat.1998.2324, available online at http://www.idealibrary.com on IDEAL®

RESEARCH NOTE

Proton Distribution in Modified FAU-Type Zeolites

T. L. M. Maesen[1] and E. P. Hertzenberg

Zeolyst International, PQ R&D Center, 280 Cedar Grove Road, Conshohocken, Pennsylvania 19428–2240

Received June 24, 1998; revised October 27, 1998; accepted November 5, 1998

The use of temperature-programmed desorption (TPD) of isopropylamine (IPAm) was extended to quantify the Brønsted acid site distribution in various modified FAU-type zeolites. We show that while the protons in nonsteamed H-FAU zeolites are distributed evenly between the supercages and sodalite cages, steaming perturbs this distribution by generating nonframework alumina species. Usually, mild steaming reduces the supercage proton density to below 50% of the total proton density. More severe steaming and a subsequent aluminum extraction restore the even distribution.

Key Words: **isopropylamine adsorption; acid site characterization; FAU-type zeolites.**

Zeolites that contain Brønsted sites are used extensively in catalysts in the oil refining and (petro)chemical industries (1). The density of the Brønsted acid sites often dominates the catalytic activity and selectivity of these zeolites. Accordingly, quantification of the Brønsted acid site density is essential for understanding zeolite-catalyzed processes.

In the hydrogen form of FAU-type zeolites the Brønsted acid site density is traditionally quantified by assuming that it equals the number of framework aluminum atoms per unit cell. This framework aluminum density can be determined from the size of the FAU-type unit cell as determined by X-ray diffraction (XRD) (2). However, for steam-stabilized (ultrastabilized) FAU-type zeolites, the relationship between the Brønsted acid site density and the unit cell size is not accurate enough to allow an unambiguous correlation to catalytic performance (3).

The XRD quantification of Brønsted acid site density is impeded by the disorder created by the steam stabilization. Steaming a hydrogen or ammonium form of a FAU-type zeolite removes some of the framework aluminum, leaving a considerable number of vacancies (4). This not only reduces the acid site density, but also creates a lot of amorphous alumina and aluminosilicate debris. Some of the debris can be removed by a subsequent aqueous extraction step. Both the vacancies and the amorphous debris affect the unit cell size as determined by XRD (4). Accordingly, the Brønsted acid site density can no longer be described as a unique function of the unit cell size. In addition, steaming leads to the formation of cationic alumina species, which are able to exchange or react with protons. The presence of this cationic alumina further decreases the Brønsted acid site density, but leaves the framework aluminum density—and hence the unit cell size—virtually unaffected.

The intrinsic flaws in the XRD quantification of Brønsted acid site density can be overcome by monitoring the proton densities directly and in a relatively nonintrusive way with infrared spectroscopy (5), ^{1}H magic-angle spinning nuclear magnetic resonance (MAS NMR) (6, 7), or the catalytic decomposition of alkylamines during temperature-programmed desorption (TPD) (8–13). In this study we use the TPD method to quantify the proton density in modified FAU-type zeolites, and compare it with the traditional XRD method. We have used isopropylamine (IPAm) as a probe molecule.

H-FAU samples were prepared from commercial samples of CBV100 (SAR = 5.0 Na-FAU) and CP300-63 (SAR = 5.3 Na-FAU). Additionally, SAR = 9.0 Na-FAU parent samples were synthesized using tetrapropylammonium ion as a void filler (14). Each Na-FAU was converted into NH_4-FAU [having $(Na + K)/Al_{framework} \leq$ 0.05 mol/mol] by means of a potassium exchange followed by an ammonium exchange, as described elsewhere (15). The NH_4-FAU was converted into H-FAU by thermal decomposition of the ammonium ion during sample activation in the thermogravimetric analysis (TGA) apparatus during the initial part of the IPAm TPD procedure.

Silica-inserted FAU was prepared by partial removal of the framework aluminum from a partially ammonium-exchanged NH_4,Na-FAU ($SiO_2/Al_2O_3 = 5.03$ mol/mol, $Na/Al = 0.18$ mol/mol). Substitution of silicon into the FAU framework was achieved by treatment of the NH_4,Na-FAU with ammonium hexafluorosilicate (AHS) followed by a

[1] To whom correspondence should be addressed. E-mail: tmaesen@pqcorp.com.

0021-9517/99 $30.00

treatment to remove the fluorine [as described elsewhere (16)]. The resulting AHS-FAU product had a $SiO_2/Al_2O_3 = 14.9$, a unit cell size $a_0 = 2.444$ nm, and Na/Al = 0.04 mol/mol (Table 1).

US-FAU (defined by $a_0 \geq 2.440$ nm) and VUS-FAU (defined by $a_0 < 2.440$ nm) samples were made by subjecting NH_4,Na-FAU and NH_4-FAU precursors to various sets of ultrastabilization steaming conditions, followed by an (acidified) ammonium exchange or by an acid leaching step. This extraction of aluminum is called "mild" if the bulk silica-to-alumina ratio of the final product does not exceed 25 and "severe" when it does. All of the US- and VUS-FAU products had $Na/Al_{framework} < 0.04$ mol/mol.

AHS-US-FAU samples were prepared by extraction of mostly nonframework aluminum from two US-FAU samples (commercial CBV500 materials), using 0.30 g AHS per gram of US-FAU (17). A lower unit cell size was obtained using 0.45 g AHS per gram of US-FAU. The three AHS-US-FAU samples had Na/Al < 0.04 mol/mol.

XRD scans of the FAU samples were obtained using a Philips 3100 X-ray diffractometer and the procedure and calculations described in ASTM D3942, "Unit Cell Dimension of Faujasite Zeolites."

IPAm TPD measurements were made on a DuPont 951 TGA module combined with a TA Instruments Thermal Analyst 2200 controller, using high-purity He at a flow rate of 100 ml/min. Our IPAm TPD method calculates the Brønsted acid site density using the appropriate weight loss of IPAm as determined from the TGA curve of a zeolite sample (25–35 mg). The sample is first flushed (in flowing He) at 773 K, then cooled to 373 K and exposed to an IPAm-in-He stream for about 5 min. Subsequently, the IPAm dosing is switched off, and the sample is equilibrated in flowing He for 50 min. Finally, a TGA curve is recorded from 373 to 823 K, with a ramp rate of 10 K/min. At the 10 K/min desorption rate, the catalytic decomposition of IPAm on FAU occurs almost exclusively in the range 575–660 K, with a differential thermogravimetric (DTG) peak maximum at about 625–635 K. A small amount of IPAm is released intact from strong Lewis acid sites in the range 640–675 K (13), with a DTG peak maximum at about 660 K. This desorption was factored out of the total strong Brønsted acidity using the DTG curve as a reference.

Elemental analyses for sodium, aluminum, and silicon were done using X-ray fluorescence on a Philips X-unique wave dispersive spectrometer.

To allow direct comparison of the XRD and IPAm TPD acid site densities, the data generated by each method are reported in terms of the number of framework aluminum atoms per unit cell [henceforth referred to as $N(Al_{fr})$] and the number of strong Brønsted acid sites per unit cell [referred to as $N(H^+)_{IPAm}$], respectively.

The $N(Al_{fr})$ values of the three H-FAU samples have been calculated from their SiO_2/Al_2O_3 ratio, as determined by elemental analyses. The $N(Al_{fr})$ values of the AHS-FAU

TABLE 1

Characterization of the FAU-Type Zeolites by XRD, X-Ray Fluorescence, and IPAm TPD

FAU type	a_0 (nm)	SAR	$[H^+]$ (mmol/g)	$N(Al_{fr})$	$N(Al_{ext})$	$N(H^+)_{IPAm}$
H-FAU	2.475	5.0	2.27	51.9	0.0	26.2
H-FAU	2.472	5.5	2.34	51.2	0.0	27.0
US-FAU	2.458	5.7	1.61	40.4	4.4	18.6
US-FAU	2.458	7.0	1.17	40.1	8.5	13.5
US-FAU	2.458	6.3	1.04	40.1	5.0	12.0
US-FAU	2.457	6.9	1.19	39.0	8.1	13.7
H-FAU	2.456	9.0	1.64	35.0	0.0	18.9
US-FAU	2.456	7.3	1.47	37.9	9.9	17.0
US-FAU	2.453	6.3	1.42	34.3	8.5	16.4
US-FAU	2.452	7.8	1.22	33.4	15.4	14.1
US-FAU	2.452	5.0	1.21	33.4	0.0	14.0
US-FAU	2.451	7.7	1.20	32.3	11.6	13.8
US-FAU	2.451	5.4	1.02	32.3	0.0	11.8
US-FAU	2.450	6.3	1.16	31.6	8.6	13.4
US-FAU	2.450	5.2	1.08	31.2	1.3	12.5
US-FAU	2.450	7.0	1.40	31.1	12.1	16.1
US-FAU	2.449	9.0	1.22	30.0	16.3	14.1
AHS-FAU[a]	2.449	11.2	0.88	34.2	22.2	10.1
US-FAU	2.448	6.9	0.82	28.7	8.2	9.4
US-FAU	2.447	5.7	0.97	27.8	4.8	11.2
US-FAU	2.445	6.4	1.07	25.1	9.1	12.3
AHS-FAU	2.444	14.9	1.31	28.7	nd[b]	15.1
AHS-US-FAU	2.442	16.1	1.06	22.2	nd	12.2
AHS-US-FAU	2.441	16.5	1.10	21.1	nd	12.7
US-FAU	2.441	6.0	0.73	20.8	6.3	8.4
VUS-FAU	2.439	5.7	0.64	18.8	4.8	7.4
VUS-FAU	2.435	9.5	0.56	14.3	17.8	6.5
VUS-FAU	2.435	6.1	0.64	14.3	7.2	7.4
AHS-US-FAU	2.434	28	0.74	13.2	nd	8.5
VUS-FAU	2.434	12.8	0.68	13.2	25.3	7.8
VUS-FAU	2.434	8.3	0.61	13.2	17.3	7.0
VUS-FAU	2.434	5.7	0.46	13.2	4.8	5.3
VUS-FAU	2.433	7.4	0.39	12.1	13.8	4.5
VUS-FAU	2.432	9.8	0.63	11.0	18.7	7.3
VUS-FAU	2.432	9.6	0.59	11.0	18.1	6.8
VUS-FAU	2.432	9.4	0.64	11.0	20.9	7.4
VUS-FAU	2.432	9.2	0.47	11.0	20.3	5.4
VUS-FAU	2.432	9.6	0.45	10.8	18.2	5.2
VUS-FAU	2.431	7.0	0.34	9.9	12.0	3.9
VUS-FAU	2.430	10.1	0.50	8.7	19.5	5.8
VUS-FAU	2.429	20	0.22	7.8	33.7	2.5
VUS-FAU	2.429	11.4	0.42	7.6	26.0	4.8
VUS-FAU	2.429	10.5	0.29	7.6	23.9	3.3
VUS-FAU	2.428	38	0.28	6.5	45.0	3.2
VUS-FAU	2.428	10.0	0.28	6.5	22.6	3.2
VUS-FAU	2.428	7.0	0.27	6.5	12.0	3.1
VUS-FAU	2.428	7.0	0.26	6.5	12.0	3.0
VUS-FAU	2.427	13.8	0.12	5.4	26.9	1.4
VUS-FAU	2.427	10.2	0.34	5.4	23.1	3.9
VUS-FAU	2.427	10.0	0.31	5.4	22.6	3.6
VUS-FAU	2.427	30	0.13	5.3	39.2	1.5
VUS-FAU	2.427	60	0.09	4.9	45.0	1.0
VUS-FAU	2.426	82	0.05	4.3	46.6	0.6
VUS-FAU	2.426	7.0	0.17	4.3	12.0	2.0
VUS-FAU	2.426	7.0	0.14	4.3	12.0	1.6
VUS-FAU	2.425	85	0.07	3.4	46.8	0.8
VUS-FAU	2.424	70	0.07	2.5	45.9	0.8
VUS-FAU	2.424	139	0.04	2.0	51.9	0.5

[a] From the literature (10).
[b] Not determined.

samples have been calculated from the unit cell size [referred to as a_0 (nm)] according (4, 18) to:

$$N(\mathrm{Al_{fr}}) = 1152 \cdot (a_0 - 2.4191). \quad [1]$$

To calculate the $N(\mathrm{Al_{fr}})$ values from the unit cell size of FAU samples that had been steamed at some point in their preparation (namely, US-FAU, AHS-US-FAU, and VUS-FAU) a different relationship has to be used, because a steamed FAU framework is significantly less ordered than a nonsteamed FAU (2, 4):

$$N(\mathrm{Al_{fr}}) = 1121 \cdot (a_0 - 2.4222). \quad [2]$$

Thus, a US-FAU can now be redefined by $N(\mathrm{Al_{fr}}) \geq 20$, and a VUS-FAU by $N(\mathrm{Al_{fr}}) < 20$.

We quantify the change in bulk SiO_2/Al_2O_3 ratio [referred to as SAR (mol/mol)], caused by the aluminum extraction to make US-FAU and VUS-FAU, as aluminum atoms per unit cell (referred to as $N(\mathrm{Al_{extr}})$).

The $N(H^+)_{\mathrm{IPAm}}$ values are calculated from the acid site concentration (i.e., $[H^+]$ in mmol/g) and the SAR (mol/mol) as

$$N(H^+)_{\mathrm{IPAm}} = \frac{[H^+]}{1000} \cdot \frac{192 \cdot \left((\mathrm{SAR}/2) \cdot M_{SiO_2} + M_{HAlO_2}\right)}{\mathrm{SAR}/2 + 1}. \quad [3]$$

In this formula $M_{SiO_2} = 60.08$ g/mol and $M_{HAlO_2} = 59.99$ g/mol are the molecular weights of framework SiO_2 and $HAlO_2$, respectively. Thus, the second factor in formula [3] calculates the weight of a FAU-type unit cell, not taking into account the compositional variation in the nonframework alumina.

The $N(\mathrm{Al_{fr}})$ and $N(H^+)_{\mathrm{IPAm}}$ values are tabulated in Table 1.

Comparing the IPAm TPD results of the three H-FAU samples [with $35 \leq N(\mathrm{Al_{fr}}) < 52$] shows that the $N(H^+)_{\mathrm{IPAm}}$ value is $52 \pm 2\%$ of the $N(\mathrm{Al_{fr}})$ value (Table 1, Fig. 1). A (nonspecified) discrepancy between $N(H^+)_{\mathrm{IPAm}}$ and $N(\mathrm{Al_{fr}})$ in nonsteamed FAU was reported earlier (9). It was attributed to the inability of the protons in the sodalite cage to catalyze the decomposition of the IPAm probe and so contribute significantly to the $N(H^+)_{\mathrm{IPAm}}$ value (9, 10). Accordingly, the difference between $N(H^+)_{\mathrm{IPAm}}$ and $N(\mathrm{Al_{fr}})$ indicates that approximately 50% of all the protons reside inside the supercages. Since protons reside in either the supercage or the sodalite cage (5, 7, 19), the other 50% has to be inside the sodalite cages. Powder neutron diffraction (19), ^{1}H MAS NMR (7) and infrared spectroscopy (5) data on H-FAU corroborate this proposed distribution of the protons between sodalite cages and supercages. Accordingly, in the case of the H-FAU where $35 \leq N(\mathrm{Al_{fr}}) < 52$, our $N(H^+)_{\mathrm{IPAm}}$ value appears to represent, quantitatively, only the protons in the supercages and none of the ones in the sodalite cages.

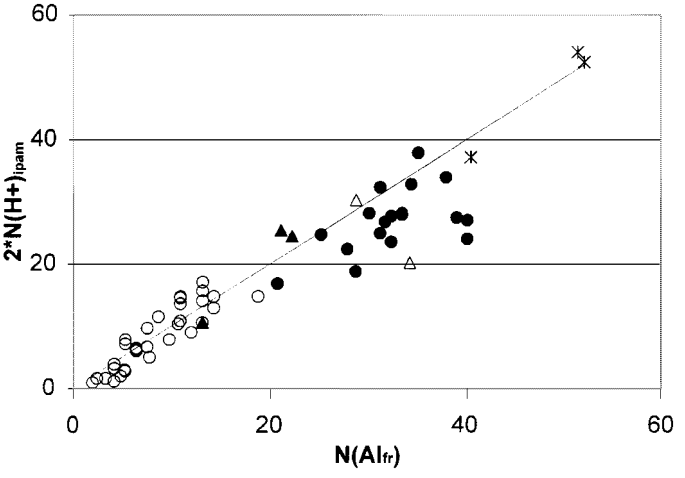

FIG. 1. Variation of the acid site density $[2 * N(H^+)_{\mathrm{IPAm}}]$ with the framework aluminum density $[N(\mathrm{Al_{fr}})]$ for H-FAU (∗), AHS-FAU (△), AHS-US-FAU (▲), US-FAU (●), and VUS-FAU (○). The straight line connects the points where $2 * N(H^+)_{\mathrm{IPAm}} = N(\mathrm{Al_{fr}})$.

To see if the proton distribution in FAU changes at $N(\mathrm{Al_{fr}}) < 35$, we included an AHS-FAU with $N(\mathrm{Al_{fr}}) = 29$ in our study. As with H-FAU, the AHS-FAU should have all the supercage acid sites available for reactions (4, 17) such as IPAm decomposition. IPAm TPD on this AHS-FAU sample yields $N(H^+)_{\mathrm{IPAm}} = 15$, consistent with the proton distribution found for H-FAU with $35 \leq N(\mathrm{Al_{fr}}) < 52$. In marked contrast, an IPAm TPD study in the literature (10) reports an $N(H^+)_{\mathrm{IPAm}}$ value of only 10 for an AHS-FAU sample with $N(\mathrm{Al_{fr}}) = 34$ (calculated by formula [1] and included in Fig. 1 and Table 1). This would be a significant deviation from the proton distributions we have found. A possible explanation for the low $N(H^+)_{\mathrm{IPAm}}$ in the literature AHS-FAU sample is the recipe used to make AHS-FAU; no special care was taken to eliminate the cationic aluminum fluoride species that are formed during the AHS treatment. These cations can easily occupy acid sites, thereby preventing such a site from catalyzing the decomposition of IPAm. In contrast, we added an extra washing step (16) with aqueous Al^{3+} to make sure these species were washed out, and subsequently found an $N(H^+)_{\mathrm{IPAm}}$ value closer to the expected $0.5 * N(\mathrm{Al_{fr}})$.

AHS-US-FAU represents a class of samples somewhat more complicated than AHS-FAU (or H-FAU). Similar to US-FAU, the framework of AHS-US-FAU has been rendered less ordered by a steam stabilization treatment. In contrast to US-FAU though, most of the supercage acid sites in AHS-US-FAU are available for reaction (17). IPAm TPD of the three AHS-US-FAU samples shows a $N(H^+)_{\mathrm{IPAm}}$ value that is 50% of $N(\mathrm{Al_{fr}})$ (Table 1), suggesting that the steaming and mild leaching followed by an AHS treatment do not perturb the proton distribution as we have observed in H-FAU and AHS-FAU samples.

Since we consistently find that the supercage proton densities approach 50% of the framework aluminum densities in FAU-type zeolite samples with little if any nonframework alumina, we plotted $2 * N(H^+)_{IPAm}$ against $N(Al_{fr})$ for all FAU samples (Fig. 1). We added a line representing $2 * N(H^+)_{IPAm} = N(Al_{fr})$, and we included data for the US-FAU and VUS-FAU samples. Figure 1 suggests that the supercage proton density of VUS-FAU samples [i.e., for $N(Al_{fr}) < 20$] approaches 50% of the framework aluminum density, similar to that in nonsteamed H-FAU and AHS-FAU. A similar correlation between the Brønsted acid site density and framework aluminum density was previously reported for VUS-FAU using *n*-propylamine TPD (8). Surprisingly, variations in the nonframework aluminum density in the VUS-FAU zeolites (Table 1) do not significantly affect this correlation (Fig. 1), indicating that virtually all supercage protons are freely accessible.

In contrast to VUS-FAU zeolites, US-FAU zeolites [i.e., having $20 \leq N(Al_{fr}) < 45$] generally show a supercage proton density significantly lower than 50% of the framework aluminum density (Fig. 1), indicating a significant blockage or removal of supercage acid protons by debris (nonframework alumina and some amorphous aluminosilicate). Apparently, the supercages of US-FAU contain significantly more debris than those of VUS-FAU.

The debris in the supercages of US-FAU and VUS-FAU can be attributed to either the steaming or the aluminum extraction step used in forming these materials. To examine the effect of the aluminum extraction step, we compare the measured reduction in supercage proton density [quantified by $N(Al_{fr}) - 2 * N(H^+)$] with the number of aluminum atoms per unit cell that were extracted [i.e., $N(Al_{ext})$]. There appears to be no definitive relationship between the $N(Al_{ext})$ and $N(Al_{fr}) - 2 * N(H^+)$ values (Fig. 2). Thus, the extraction step has only a limited effect on the release of debris from supercage acid sites.

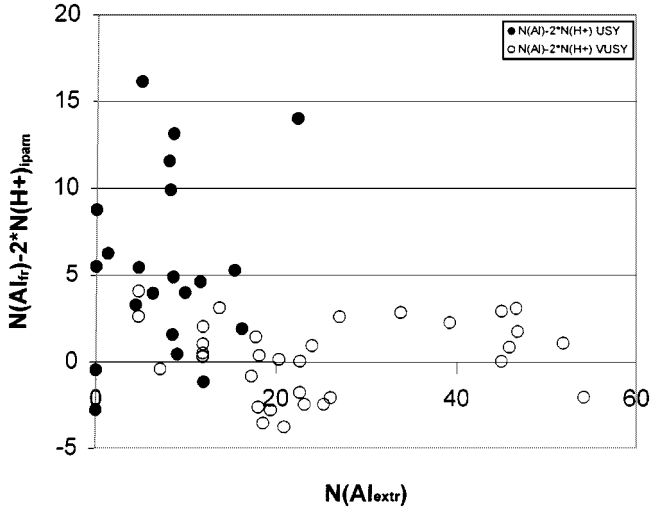

FIG. 2. Impact of the amount of aluminum extracted $N(Al_{fr})$ on the difference between framework aluminum density and acid site density $N(Al_{fr}) - 2 * N(H^+)_{IPAm}$ for US-FAU (●) and VUS-FAU (○).

An explanation for the relatively large amount of debris in the US-FAU supercages (as compared with those of VUS-FAU) is that after mild steaming and extraction (to make US-FAU), the supercages still contain most of the alumina just after it has been released from the framework. During the more severe steaming (to make VUS-FAU), the nonframework alumina has had a chance to diffuse toward the outer crystal surface, and after a subsequent extraction step, the remaining nonframework alumina no longer interferes with the supercage Brønsted acid sites. Interestingly, IPAm TPD allows quantification of the reduction in the number of accessible acid sites due to the presence of intracrystalline debris.

In summary, we have shown that IPAm TPD can be used to determine the proton distribution between supercage and sodalite cage sites in variously modified FAU-type zeolites. This cannot be done by other nonintrusive techniques such as IR spectroscopy and ^{1}H NMR.

ACKNOWLEDGMENTS

The authors thank J. McManus for conducting the IPAm TPD experiments; A. Moñino for her assistance in sample preparation; A. Marchese, M. Kohl, F. Graziano, and A. Marcus for their XRD and XRF work; and M. S. Rigutto and R. J. Hinchey for many helpful discussions.

REFERENCES

1. Maxwell, I. E., and Stork, W. H. J., *in* "Introduction to Zeolite Science and Practice" (H. van Bekkum, E. M. Flanigen, and J. C. Jansen, Eds.), Stud. Surf. Sci. Catal., Vol. 58, p. 571. Elsevier, Amsterdam, 1991.
2. Kerr, G. T., *Zeolites* **9**, 350 (1989).
3. Bezman, R. D., *Catal. Today* **13**, 143 (1992).
4. Szostak, R., *in* "Introduction to Zeolite Science and Practice" (H. van Bekkum, E. M. Flanigen, and J. C. Jansen, Eds.), Stud. Surf. Sci. Catal., Vol. 58, p. 153. Elsevier, Amsterdam, 1991.
5. Makarova, M. A., Ojo, A. F., Karim, K., Hunger, M., and Dwyer, J., *J. Phys. Chem.* **98**, 3619 (1994).
6. Shertukde, P. V., Hall, W. K., Dereppe, J.-M., and Marcelin, G., *J. Catal.* **139**, 468 (1993).
7. Brunner, E., *Microporous Mater.* **1**, 431 (1993).
8. Biaglow, A. I., Gittleman, C., Gorte, R. J., and Madon, R. J., *J. Catal.* **129**, 88 (1991).
9. Biaglow, A. I., Parrillo, D. J., and Gorte, R. J., *J. Catal.* **144**, 193 (1993).
10. Biaglow, A. I., Parrillo, D. J., Kokotailo, G. T., and Gorte, R. J., *J. Catal.* **148**, 213 (1994).
11. Farneth, W. E., and Gorte, R. J., *Chem. Rev.* **95**, 615 (1995).
12. Juskelis, M. V., Slanga, J. P., Roberie, R. G., and Peters, A. W., *J. Catal.* **138**, 391 (1992).
13. Kanazirev, V., Dooley, K. M., and Price, G. L., *J. Catal.* **146**, 228 (1994).
14. Vaughan, D. E. W., and Strohmaier, K. G., U.S. Patent 4,931,267, 1990.
15. Cooper, D. A., WO 9503248, 1995.
16. Hinchey, R. J., and Caglione, A. J., U.S. Patent 4,597,956, 1986.
17. Corma, A., Fornés, V., and Rey, F., *Appl. Catal.* **59**, 267 (1990).
18. Zi, G., and Yi, T., *Zeolites* **8**, 232 (1988).
19. Czjzek, M., Jobic, H., Fitch, A. N., and Vogt, T., *J. Phys. Chem.* **96**, 1535 (1992).